

ON THE BOLOMETRIC QUIESCENT LUMINOSITY AND LUMINOSITY SWING OF BLACK HOLE CANDIDATE AND NEUTRON STAR LOW MASS X-RAY TRANSIENTS

SERGIO CAMPANA

Osservatorio Astronomico di Brera, Via Bianchi 46, I-23807 Merate (LC), Italy,
e-mail: campana@merate.mi.astro.it

AND

LUIGI STELLA

Osservatorio Astronomico di Roma, Via Frascati 33, I-00040 Monteporzio Catone (Roma), Italy,
e-mail: stella@coma.mporzio.astro.it

Draft version October 29, 2018

ABSTRACT

Low mass X-ray transients hosting black hole candidates display on average a factor of ~ 100 larger swing in the minimum (quiescent) to maximum (outburst) X-ray luminosity than neutron star systems, despite the fact that the swing in the mass inflow rate is likely in the same range. Advection dominated accretion flows, ADAFs, were proposed to interpret such a difference, because the advected energy disappears beyond the event horizon in black hole candidates, but must be radiated away in neutron star systems. The residual optical/UV emission of quiescent low mass X-ray transients, after subtraction of the companion star spectrum, was originally ascribed to optically thick emission from the outer accretion disk regions, where matter accumulates. Difficulties with this interpretation, led to a revised ADAF model where the bulk of the residual optical/UV emission in quiescence does not originate in the outermost disk regions but is instead produced by synchrotron radiation in the ADAF, and therefore is part of the ADAF's luminosity budget. We demonstrate that, once the residual optical/UV emission is taken into account, the bolometric luminosity swing of black hole candidates is consistent with that of neutron star systems. Therefore ascribing the bulk of the residual optical/UV flux to the ADAF removes much of the evidence on which ADAF models for low mass X-ray transients were originally developed, namely the higher luminosity swing in black holes than in neutron stars. We also find that, for the neutron star spin periods (a few ms) and magnetic fields ($\sim 10^8 - 10^9$ G) inferred from some low mass X-ray transients, the mass to radiation conversion efficiency of recently proposed ADAF/propeller models is considerably higher than required to match the observations, once the contribution from accretion onto the magnetospheric boundary is taken into account. Motivated by these findings, we explore here an alternative scenario to ADAFs in which very little mass accretion onto the collapsed star (if at all) takes place in the quiescence intervals, whereas a sizeable fraction of the mass being transferred from the companion star (if not all) accumulates in an outer disk region. As in some pre-ADAF models, the residual optical/UV emission of black hole candidate systems are expected to derive from the gravitational energy released by the matter transferred from the companion star at radii comparable to the circularisation radius. The quiescent X-ray luminosity originates either from accretion onto the black hole candidates at very low rates and/or from coronal activity in the companion star or in the outer disk. For comparably small mass inflow rates, it can be concluded that the neutron stars in these systems are likely in the radio pulsar regime. In the interaction of the radio pulsar relativistic wind with matter transferred from the companion star, a shock forms, the power law-like emission of which powers both the harder X-ray emission component and most of the residual optical/UV observed in quiescence. The soft, thermal-like X-ray component may arise from the cooling of the neutron star surface in between outbursts or, perhaps, heating of the magnetic polar caps by relativistic particles in the radio pulsar magnetosphere. This scenario matches well both the X-ray and bolometric luminosity swing of black hole candidate as well as neutron star systems, for comparable swings of mass inflow rates toward the collapsed object.

Subject headings: X-ray: stars – Accretion, accretion disks – Black hole physics – Stars: neutron

1. INTRODUCTION

Transient X-ray binaries are characterised by a luminosity that varies over many orders of magnitude, allowing to investigate accretion onto collapsed stars over a much larger range than persistent sources. Low mass X-ray transients (LMXRTs), i.e. transients with a low mass donor star, host either a sporadically accreting black hole candidate, BHC, or a neutron star, NS (e.g. Tanaka & Shibazaki 1996; Campana et al. 1998a). The outbursts

of these transients are likely caused by an instability of the accretion disk (Cannizzo, Wheeler & Ghosh 1985; van Paradijs 1996). The increased matter inflow propagates from the outer regions of the accretion disk inwards, as testified from the observation of a delay in the increase of the X-ray flux relative to optical flux at the outburst onset of GRO J1655–40 (Hameury et al. 1997) and Aql X-1 (Shahbaz et al. 1998). When determined, the characteristics of the companion star and binary system are

usually similar across BHC and NS LMXRTs: K dwarf companion stars and orbital periods in the 2–30 hr range are common (exceptions are the BHCs GS 2023+338 with an orbital period of $P_{\text{orb}} = 155$ hr and GRO J1655–40 with $P_{\text{orb}} = 62.9$ hr). Therefore, the time-averaged mass exchange rates in these systems is expected to be comparable (Menou et al. 1999, hereafter M99). It is also plausible that the swing between minimum (quiescent) and maximum (outburst) mass inflow rates towards the collapsed object is comparable in BHC and NS LMXRTs.

Observations show that the ratio of minimum X-ray luminosity in quiescence, L_{min}^X , to maximum X-ray luminosity in outburst, L_{max}^X , is significantly smaller (a factor of about 100) in BHC than in NS LMXRTs. On average this results from both a higher L_{max}^X and a lower L_{min}^X in BHC systems (Narayan, Garcia & McClintock 1997, hereafter N97; Garcia et al. 1998, hereafter G98; M99). Eddington-limited accretion is likely responsible for the fact that only BHCs, being more massive than NSs, achieve $L_{\text{max}}^X > 10^{38.5}$ erg s $^{-1}$. N97 (see also G98 and M99) argue that the smaller values of $L_{\text{min}}^X/L_{\text{max}}^X$, as well as L_{min}^X , in BHC transients demonstrate that the mass to radiation conversion efficiency is considerably lower in quiescence, as expected for advection-dominated accretion flows, ADAFs, crossing an event horizon.

In this context, the residual optical/UV luminosity of quiescent systems, after subtraction of the contribution from the mass donor star, has been interpreted in different ways. In the original ADAF models of Narayan, McClintock & Yi (1996), the residual optical emission is supposed to originate from the outermost disk regions, where the optically thick standard model applies. Emission from the hot spot where the accretion stream from the mass donor impacts the disk likely contributes to the optical flux. Motivated by Wheeler’s (1996) argument that the effective temperature of such an outer accretion disk would be in the unstable regime (see also Lasota, Narayan & Yi 1996), Narayan, Barret & McClintock (1997) revised the original model and proposed that the residual optical/UV luminosity derives from synchrotron emission in the ADAF, while the outer standard disk region is cooler and farther from the BH, and emits mainly in the infrared (see Menou, Narayan and Lasota 1999). It should be emphasised that, in this case, besides the X-ray emission, the residual optical/UV emission should therefore be included in the energy budget of the ADAF. In Section 2 we review the X-ray and optical properties of BHCs and NSs and compare their minimum to maximum luminosity ratios with and without the inclusion of the residual optical/UV quiescent luminosity. As a result no clear distinction is found between the luminosity ratio of these two classes if the residual optical/UV luminosity is included in the budget.

In Section 3 we comment on some difficulties in the application of ADAF scenarios to quiescent BHC and NS systems. We then consider an alternative scenario for the quiescent emission of LMXRTs, which does not involve an ADAF solution. The basic ansatz of this scenario is that a very small fraction of the transferred matter (if at all) reaches the compact object during quiescence; rather most of the transferred matter is supposed to accumulate close to the circularisation radius or lost in a wind (Section 4).

As in pre-ADAF models of BHC LMXRTs, the implied ratio of quiescence to outburst mass inflow rates towards the collapsed star is $10^{-7} - 10^{-8}$ (or smaller). We show that, if the same ratio applies also to the fast spinning weakly magnetic NSs hosted in LMXRTs, then the radio pulsar regime is expected to operate in the quiescent state, with shock emission driven by the pulsar wind dominating the quiescent luminosity and spectrum of these systems. In section 5 some properties of quiescent LMXRTs are also compared with the expectations of our model. Our conclusions are summarised in Section 6.

2. BOLOMETRIC LUMINOSITIES OF QUIESCENT LOW MASS X-RAY TRANSIENTS

We estimate here the quiescent optical/UV luminosity of LMXRTs once the contribution from the mass donor star is subtracted (see also Menou, Narayan & Lasota 1999). We adopt the source sample and X-ray luminosities (0.5–10 keV range) of G98, complemented with recent results on the NS systems SAX J1808.4–3658 (Stella et al. 2000) and X 1732–304 (Guainazzi et al. 1999). Our results remain unchanged if the X-ray luminosities derived by C97 are used in place of those in G98 (see also Tab. 1 and Fig. 1). Being many orders of magnitude higher than the optical luminosity, the maximum X-ray luminosity provides a reliable estimate of the bolometric luminosity at the outburst peak (i.e. $L_{\text{max}}^X = L_{\text{max}}^{\text{bol}} = L_{\text{max}}$). Optical V magnitudes and absorptions are from C97, unless otherwise specified.

2.1. Black hole candidates

The BHC transient A 0620–00 has a quiescent 0.5–10 keV luminosity of $L_{\text{min}}^X \sim 10^{31}$ erg s $^{-1}$ (for a distance of 1.2 kpc). This value is obtained by extrapolating the ROSAT data and using a fixed column density of $N_H = 1.2 \times 10^{21}$ cm $^{-2}$ (McClintock et al. 1995). Due to the small number of collected photons in the ROSAT observation (~ 40) the spectrum is very poorly determined and can be well fit by a variety of single component models. A short wavelength HST/FOS spectrum of the quiescent optical counterpart yielded a 1350–2200 Å luminosity of $0.6 - 4 \times 10^{31}$ erg s $^{-1}$. These results have been confirmed by higher quality HST/STIS spectra (McClintock & Remillard 2000). At optical wavelengths (2200–4750 Å) the spectrum can be fit by a 9000 K black body (luminosity of $\sim 10^{32}$ erg s $^{-1}$), after subtraction of the $58 \pm 4\%$ contribution from the K5V star companion, which affects mainly the spectrum at wavelengths $\gtrsim 4000$ Å. At longer wavelengths (2.0–2.5 μm) the K dwarf flux dominates, making up $75 \pm 17\%$ of the infrared luminosity (Shahbaz et al. 1999). Therefore, the quiescent optical/UV luminosity of A 0620–00 outshines the X-ray luminosity by a factor of ~ 10 (see also McClintock et al. 1995). We estimate a rough bolometric quiescent luminosity of $L_{\text{min}}^{\text{bol}} \sim 10^{32}$ erg s $^{-1}$.

The lowest quiescent X-ray luminosity detected from GS 2023+338 (V 404 Cyg) is $L_{\text{min}}^X \sim 2 \times 10^{33}$ erg s $^{-1}$ (Narayan, Barret & McClintock 1997; Campana 2000). The spectrum is well fit by either a power law (photon index $\Gamma \sim 1.5 - 2$) or a bremsstrahlung ($kT_{\text{br}} \sim 5 - 10$ keV). GS 2023+338 is significantly reddened ($A_V \sim 4$ mag) and no UV data are available. Casares et al. (1993) estimate that the contribution of the accretion disk to

TABLE 1
TABLE 1: LUMINOSITIES* OF LMXRTs (SEE TEXT).

Name	P_{orb} (hr)	d (kpc)	$\log L_{\text{min}}^X$ (erg s^{-1})	$\log L_{\text{min}}^{\text{opt}}$ (erg s^{-1})	$\log L_{\text{min}}^X$ (erg s^{-1}) [◊]	$\log L_{\text{max}}$ (erg s^{-1})	$\log L_{\text{circ}}$ (erg s^{-1})
GROJ0422+32	5.1	3.6	< 31.9	31.7	~ 32.1	37.9 (37.8)	32.4
A 0620-00	7.8	1.2	31.0	32.0	32.0	38.4 (38.1)	32.3
GS 2000+25	8.3	2.7	< 32.3	32.6	~ 32.8	38.4 (38.3)	32.4
GS 1124-684	10.4	6.5	< 32.6	32.3	~ 32.8	39.1 (38.9)	32.1
H 1705-250	16.8	8.6	< 33.7	34.4	~ 34.5	38.3 (39.6)	32.5
4U 1543-47	27.0	8.0	< 33.7	34.6	~ 34.7	39.6 (39.0)	33.2
GROJ1655-40	62.9	3.2	32.4	33.6	33.6	38.5 (38.1)	33.5
GS 2023+338	155.3	3.5	33.2	34.3	34.3	39.3 (39.3)	33.3
SAX J1808.4-3658	2.0	4.0	32.5	< 32.6	~ 32.5	36.8 (—)	33.0
4U 2129+47	5.2	6.3	32.7	~ 30	32.7	38.2 (—)	31.9
Cen X-4	15.1	1.2	32.7	32.2	32.8	38.1 (38.0)	32.0
Aql X-1	18.9	2.5	32.8	≤ 32	~ 32.8	37.6 (37.6)	32.0
4U 1608-52	—	3.3	33.3	≤ 32.3	33.3	38.0 (37.7)	—
X 1732-304	—	4.5	33.1 [†]	—	33.1	37.8 (—)	—
EXO 0748-676	3.8	3.8	34.0	~ 30	34.0	37.5 (37.3)	32.4

* Distances are from G98 (see also the text). L_{min}^X is the quiescent 0.5–10 keV luminosity, $L_{\text{min}}^{\text{opt}}$ the quiescent optical/UV luminosity after subtraction of the contribution from the companion star and $L_{\text{min}}^{\text{bol}}$ the quiescent *bolometric* luminosity as estimated from the sum of L_{min}^X and $L_{\text{min}}^{\text{opt}}$. L_{max} is the maximum luminosity, as inferred from the 0.5–10 keV luminosity at the outburst peak (see G98); values in parentheses are from Chen, Shrader & Livio (1997; hereafter C97). L_{circ} is the energy released by accretion at the circularisation radius, according to standard mass transfer models.

◊ In those cases in which the upper limits on the X-ray luminosity is larger or comparable to the measured residual optical/UV luminosity after subtraction of the contribution from the companion star, we have adopted the latter value for the bolometric luminosity.

† 2–10 keV luminosity.

the optical flux relative to the G9V–K0III companion is 72%, 36% and 19% in the B, V and R bands, respectively. These fractions convert to dereddened luminosities of $L_B \sim 8 \times 10^{33} \text{ erg s}^{-1}$, $L_V \sim 8 \times 10^{33} \text{ erg s}^{-1}$ and $L_R \sim 6 \times 10^{33} \text{ erg s}^{-1}$. For GS 2023+338 we therefore adopt a value of $L_{\text{min}}^{\text{bol}} \sim 2 \times 10^{34} \text{ erg s}^{-1}$, which is a factor of ~ 10 higher than L_{min}^X .

GRO J1655-40 has been detected in quiescence at a level of $L_{\text{min}}^X \sim 2 \times 10^{32} \text{ erg s}^{-1}$ (Hameury et al. 1997). The spectrum can be described by a power law model ($\Gamma \sim 1.5$). Soft X-ray and UV flux measurement are severely hampered by a large absorption ($A_V \sim 4 \text{ mag}$). The F5IV companion star outshines the disk in the optical ($95 \pm 2\%$ at 5500 Å; Orosz & Bailyn 1997). An estimate of the V-band luminosity of the accretion disk based on the model by Orosz & Bailyn (1997) yields $L_V \sim 4 \times 10^{33} \text{ erg s}^{-1}$. The optical quiescent luminosity therefore dominates the X-ray emission by a factor of ~ 10 .

For all other known BHC transients there are only upper limits to their quiescent X-ray flux (see Tab. 1). Yet, their optical counterparts are relatively well studied and the residual optical flux can be estimated. In particular, Keck spectra were used to estimate the fraction of the 6600–6800 Å luminosity that originates from the companion star. This is 85%, 95%, 30% and 60% in GS 1124-684 (Nova Mus 91), GS 2000+25 (Nova Vul 88), H 1705-250 (Nova Oph 77) and GRO J0422+32 (Nova Per 92), respectively (Casares et al. 1997; Harlaftis et al. 1996, 1997, 1999). All these BHCs have K–M dwarf companions. V-

magnitudes are V = 20.5, 21.2, 21.3 and 22.2 mag, respectively. By assuming that the same fractions above hold for the V band, a very conservative assumption for K–M dwarf stars, we infer that the dereddened V luminosities of the accretion disk are $L_V = 2 \times 10^{32}$, 4×10^{32} , 2×10^{34} and $5 \times 10^{31} \text{ erg s}^{-1}$, respectively. The optical counterpart of 4U 1543-47, an A2V star, has V=16.7. Orosz et al. (1998) estimate a disk contribution of 10%, 21%, 32% and 39%, in the B, V, R and I bands, respectively. The increasing disk contribution for longer optical wavelengths is due to the relatively hot companion. The dereddened disk V and I luminosities are $L_V \sim 3 \times 10^{34} \text{ erg s}^{-1}$ and $L_I \sim 10^{34} \text{ erg s}^{-1}$, respectively. Consequently we estimate $L_{\text{min}}^{\text{bol}} \sim 4 \times 10^{34} \text{ erg s}^{-1}$.

Therefore, we conclude that the bolometric luminosity of quiescent BHC LMXRTs is dominated by optical/UV disk emission. When both the X-ray and optical quiescent luminosities are available, the latter are systematically higher by about an order of magnitude.

2.2. Neutron stars

The two best studied NS LMXRTs, Aql X-1 and Cen X-4, have $L_{\text{min}}^X \sim 6 \times 10^{32} \text{ erg s}^{-1}$ (Campana et al. 1998b) and $L_{\text{min}}^X \sim 5 \times 10^{32} \text{ erg s}^{-1}$ (Asai et al. 1998; Campana et al. 2000), respectively. Recent optical studies of the field of Aql X-1 indicate that the true optical counterpart is located 0.5'' from the previously known star (e.g. Shahbaz, Casares & Charles 1997). The magnitude of the counterpart is V = 21.6 mag (Chevalier et al. 1999). The dereddened ($A_V = 1.2 \text{ mag}$) V luminosity can therefore be $L_V \sim 10^{32} \text{ erg s}^{-1}$ at the most (i.e. if the entire V

luminosity came from the disk). In any case this luminosity represents a small fraction of the quiescent X-ray luminosity.

In the case of Cen X-4 the residual optical flux is estimated to contribute 80%, 30%, 25% and 10% in the B, V (18.7 mag), R and I bands, respectively (Shahbaz, Naylor & Charles 1993). The corresponding reddening-corrected luminosities ($A_V = 0.3$ mag) are $L_B \sim 9 \times 10^{31}$ erg s $^{-1}$, $L_V \sim 5 \times 10^{31}$ erg s $^{-1}$, $L_R \sim 6 \times 10^{31}$ erg s $^{-1}$ and $L_I \sim 2 \times 10^{31}$ erg s $^{-1}$. Recently, an UV spectrum has been obtained with the HST/STIS (McClintock & Remillard 2000). The main result is that in a νF_ν vs. ν representation there is only factor of $\sim 1 - 2$ increase from the X-rays to the optical. Therefore, the quiescent X-ray and optical luminosities are comparable in Cen X-4.

The quiescent X-ray state of these two sources has been studied in some detail with BeppoSAX and ASCA pointed observations. Their 0.1–10 keV spectrum comprises a soft component, modeled by a black body with $kT_{\text{bb}} \sim 0.1 - 0.3$ keV and equivalent radius of $\sim 1 - 3$ km, plus a hard power law component with photon index $\sim 1 - 2$ (Campana et al. 1998b, 2000; Asai et al. 1996, 1998). The contribution of the two spectral components to the 0.5–10 keV luminosity is comparable.

The quiescent X-ray flux of 4U 1608–522, 4U 2129+47 and EXO 0748–676 has also been detected (e.g. Campana et al. 1998a, see Tab. 1). 4U 1608–522 has been revealed in quiescence at a level of $L_{\text{min}}^X \sim 2 \times 10^{33}$ erg s $^{-1}$ (0.5–10 keV for $d = 3.3$ kpc; Asai et al. 1998). The highly absorbed ($A_V = 5.2$ mag) optical counterpart of 4U 1608–522 has $J = 18.0$ mag ($R > 22$ mag) and a luminosity of $\sim 2 \times 10^{32}$ erg s $^{-1}$ at the most (including the companion star). 4U 2129+47 has $L_{\text{min}}^X \sim 6 \times 10^{32}$ erg s $^{-1}$ (0.5–10 keV for $d = 6.3$ kpc). The F9 subgiant companion dominates the optical flux ($V=18.5$ mag). Garcia & Callanan (1999) estimate $V = 24.5$ mag for the disk of 4U 2129+47, implying a dereddened ($A_V \sim 1.5$ mag) V luminosity of only $\lesssim 10^{30}$ erg s $^{-1}$. EXO 0748–676 has a relatively high quiescent luminosity of $L_{\text{min}}^X \sim 10^{34}$ erg s $^{-1}$ (0.5–10 keV for $d = 3.8$ kpc). However, being a high inclination system, EXO 0748–676 should be treated with caution since its X-ray flux variations might be driven by geometrical effects (e.g. obscuration by a variable height of the disk rim) rather than genuine mass inflow rate variations. Optical observations provided an upper limit on the V-magnitude of the quiescent optical counterpart of EXO 0748–676 ($V > 23$ mag for $A_V = 1.2$ mag); this translates to a V luminosity of $\sim 10^{30}$ erg s $^{-1}$.

In addition to the sources in the G98 sample, SAX J1808.4–3658 (Stella et al. 2000) and X 1732–304 (Guainazzi et al. 1999) have also been detected in quiescence. SAX J1808.4–3658 has a quiescent X-ray luminosity of $2 - 3 \times 10^{32}$ erg s $^{-1}$. The optical counterpart was detected only during the outburst decay. An upper limit on the quiescent V magnitude of > 20.5 mag has been derived (Giles et al. 1999). By using the galactic column density to estimate A_V , we derive an upper limit to the V luminosity of 4×10^{32} erg s $^{-1}$. X 1732–304 in the globular cluster Terzan 1 was previously considered a persistent (though highly variable) source. In April 1999 it was observed in a quiescent state at a 2–10 keV luminosity of 1.4×10^{33} erg s $^{-1}$. The quiescent X-ray spectrum was compatible with the two-component spectrum inferred

for Aql X-1 and Cen X-4. The optical counterpart is not known.

All the data above indicate that in quiescent NS LMXRTs the X-ray luminosity exceeds (or, at the most, is comparable to) the optical luminosity.

2.3. Comparison of luminosity ratios and quiescent luminosities

The ratio of minimum to maximum luminosity of LMXRTs, as estimated by N97 and G98 on the basis of the X-ray data alone, is plotted in the left panel of Fig. 1, versus the maximum luminosity. BHCs are clearly separated from NSs both in terms of maximum luminosity and X-ray luminosity ratio. The middle panel shows instead $L_{\text{min}}^{\text{bol}}/L_{\text{max}}$ as estimated above based on both X-ray and optical measurements (see also Tab. 1): the distinction between BHC and NS systems is no longer apparent. Using a Kolmogorov-Smirnov, KS, test we estimate that the values of $L_{\text{min}}^{\text{bol}}/L_{\text{max}}$ for the two classes of transients have a 9% probability of being drawn by chance from the same parent distribution (note that using the X-ray data alone the KS probability is $< 0.2\%$). To check that this conclusion is robust and independent of the method for estimating L_{max} adopted by G98, we calculated also the minimum to maximum luminosity ratios by using the L_{max} values derived by C97 (see also Tab. 1). The results are shown in the right panel of Fig. 1. Also in this case, it is not possible to distinguish BHC from NS systems by using $L_{\text{min}}^{\text{bol}}/L_{\text{max}}$ (KS probability of 22%). We note that the conclusions above are even strengthened if EXO 0748–676, and/or SAX J1808.4–3658 and X 1732–304 (i.e. the sources not included in the G98 sample) are excluded from the source sample.

Considering minimum bolometric luminosities only, one has that the BHC and NS transients population have a 56% probability of being drawn by chance from the same parent distribution. This probability is 22% if minimum bolometric luminosities in Eddington units are used instead. This is at variance with the results obtained by M99, who used minimum X-ray luminosities.

These results show that once the contribution from the optical luminosity (after subtraction of the mass donor's spectrum) is included in the evaluation of the quiescent luminosity of LMXRTs, there is no evidence that the luminosity swing of BHCs is larger than that of NSs, neither that the minimum (quiescent) luminosity of BHCs is lower. In fact the optical luminosity, while usually negligible in NS LMXRTs, dominates the quiescent luminosity of BHC transients.

3. COMMENTS ON ADAF MODELS FOR LOW MASS X-RAY TRANSIENTS

3.1. Black hole candidates

It has long been realised that, if steady accretion takes place in quiescence, standard optically thick accretion disk models (with radiative efficiency ~ 0.1) are inadequate to explain both the X-ray luminosity and the temperature vs. effective area combination inferred from the residual optical emission of BHC LMXRTs (see McClintock et al. 1995). While the former problem could be cured by invoking, e.g. the presence of a hot phase or of a Comptonising inner accretion disk region (see e.g. Spruit 2000), the latter

problem is difficult to solve: if the optically thick accretion disk extended to (or close to) the marginally stable orbit, then the area where most of the quiescent flux is emitted would be small and the corresponding black body temperature ($T_{\text{bb}} \sim 10^5 - 10^6$ K), at least, an order of magnitude higher than inferred from the residual optical emission of quiescent BHC transients (e.g. $T \sim 9000$ K in A 0620-00, see McClintock et al. 1995).

A considerable amount of work has been carried out in recent years on ADAF models, where the radiative efficiency is very low ($\sim 10^{-4} - 10^{-3}$) and most of the gravitational energy of the inflowing matter is stored as thermal and/or bulk kinetic energy and advected towards the collapsed star. Solutions of this type exist for sub-Eddington mass accretion rates ($\dot{M} < 0.1 - 0.01 \dot{M}_{\text{Edd}}$). The luminosity of an ADAF scales approximately as \dot{M}^2 (as opposed to the \dot{M} scaling of standard accretion). If the accreting object is a BH, the advected energy disappears beyond the event horizon. In the case of a NS, the energy of the ADAF is instead radiated away when the plasma reaches the star surface. This implies that, for a given swing of mass inflow rate between outburst and quiescence, the corresponding swing of accretion luminosity of BHC transients should be several orders of magnitudes larger than that of NS LMXRTs (N97). Even though the observed X-ray luminosity swing of BHCs is only a factor of ~ 100 larger than that of NS systems (whereas simple ADAF models would predict a factor of $\sim 10^3 - 10^4$) LMXRTs appeared to confirm this fundamental property of BHs accreting through an ADAF. This conclusion hinged upon the ansatz that the minimum X-ray luminosity provides a reasonable estimate of the quiescent bolometric luminosity generated by the ADAF (see N97). Indeed the ADAF model originally suggested by Narayan et al. (1996) to interpret the spectral energy distribution of the BHC transient A 0620-00 envisaged an outer optically thick standard disk (radius of $\sim 10^9$ cm), responsible for the bulk of the emitted optical/UV radiation, together with an inner ADAF giving rise to the X-ray luminosity. However, Wheeler (1996, see also Lasota, Narayan & Yi 1997) pointed out that the inferred effective temperature of the outer disk regions is within the unstable range ($\sim 5000 - 8000$ K). Moreover, it is difficult to match the advection region with the outer disk in terms of surface density and angular momentum.

A revised ADAF model was introduced by Narayan, Barret & McClintock (1997) in order to interpret the multiwavelength quiescent spectra of GS 2023+338 and eliminate the above mentioned difficulties. This model ascribes the vast majority of the optical/UV luminosity to synchrotron emission from the ADAF, which extends from a transition radius of $\sim 10^{10} - 10^{11}$ cm inwards. The outer standard disk is at larger radii and emits predominantly in the infrared. The bolometric radiative efficiency of ADAF model constructed in this way is $\sim 10^{-3}$ (as opposed to ~ 0.1 in standard accretion), with an X-ray radiative efficiency a couple of orders of magnitude lower. One of the consequences of this ADAF model is that the optical/UV emission, being produced by the ADAF, is part of the luminosity budget of the ADAF itself and should therefore be included in any comparison involving the minimum luminosity of BH and NS LMXRTs. However, the results in

Section 2 show that once the contribution from the optical/UV luminosity (after subtraction of the mass donor's spectrum) is included in the evaluation of the quiescent luminosity of LMXRTs, there is no evidence that the luminosity swing of BHCs is larger than that of NSs, neither that the minimum luminosity of BHCs is lower.

3.2. Neutron stars

Recent ADAF modeling of quiescent NS LMXRTs exploited the idea that most of the inflowing matter is prevented from reaching the NS surface by the action of the magnetospheric centrifugal barrier and that the propeller effect, ejecting matter from the magnetospheric boundary to infinity, might be at work (Zhang, Yu & Zhang 1998; M99). This was in part motivated by the growing evidence that many low mass X-ray Binaries, LMXRBs, (and likewise LMXRTs) host fast spinning NS (periods of a few ms) with weak magnetic fields ($\sim 10^8 - 10^9$ G, see Section 4.2). The fact that the observed X-ray luminosity swing of NS LMXRTs is only a factor of ~ 100 smaller than that of BHC LMXRTs played also a role. An additional issue with simple ADAF models is that, while the mass accretion rates deduced in BHC LMXRTs from ADAF modeling of their quiescent X-ray fluxes represent a large fraction ($\sim 1/3$) of the rates predicted by standard mass transfer models in binaries, the corresponding fraction in NS LMXRTs is very low ($\sim 0.1\%$; M99). This suggested that only a very small fraction of the quiescent mass inflow rate reaches the NS surface in order to power the soft (thermal-like) X-ray emission observed from several quiescent NS LMXRTs. M99 investigated in detail this possibility and concluded that an efficient propeller effect, possibly in association with mass loss in a disk wind, would be required to match the observed quiescent luminosities of NS LMXRTs.

Independent of whether the matter inflowing onto the magnetospheric boundary accumulates locally or is ejected to infinity (still an open problem), the trouble with the propeller interpretation is that there is no "sink" where the energy stored in the ADAF down to the magnetospheric radius can be permanently hidden. For the NS parameters deduced for LMXRTs, the gravitational energy, $L(r_m)$, of the accretion flow down to the magnetospheric boundary, r_m , (which must be radiated away) is large, because r_m is $\sim 10 R$ at the most, with R is the NS radius¹ (Stella et al. 1994; Campana et al. 1998a). If only a fraction of $f_R \sim 10^{-3}$ of the mass transfer rate from the companion star reaches the NS surface (M99), then $L(r_m)$ would exceed the luminosity released at the NS surface, $L(R)$, by a large factor ($R/(r_m f_R) \sim 100$). The conclusion above remains basically unchanged even if a substantial mass loss took place in the form of a disk wind. For example in the solution with the highest disk mass loss discussed by M99 (transition radius of $\sim 10^{10}$ cm, and $\dot{M}(r) \propto r^{0.8}$, i.e. their "strong wind" model), $\sim 1\%$ of the mass inflow rate reaches the magnetospheric boundary implying that $L(r_m)$ exceeds $L(R)$ by a factor of ~ 30 . (This factor would be higher still for disk models with smaller mass loss.) In principle, a possible way out could be that $L(r_m)$ is released away from the X-ray band at energies that are not accessible to current instrumenta-

¹ r_m must be smaller than the light cylinder radius.

tion. The luminosity released by the ADAF at r_m (some $10^{34} - 10^{35}$ erg s $^{-1}$) together with the size of the emitting region (roughly $r_m^2 \sim 10^{14}$ cm 2), would imply a minimum emission temperature of $\sim 0.1 - 0.2$ keV. Therefore this luminosity could not be hidden in the EUV; emission at γ -ray energies would instead be required in order to avoid detection by current instrumentation. We regard this as contrived and conclude that current ADAF/propeller models for NS LMXRTs do not appear to produce a sufficiently marked reduction of the accretion to radiation conversion efficiency to match the observations.

4. AN ALTERNATIVE SCENARIO FOR QUIESCENT LOW MASS X-RAY TRANSIENTS

As noted by a number of authors, a considerable luminosity is produced in quiescent LMXRTs by the release of gravitational energy, as the stream of matter from the Lagrangian point of the mass donor star reaches the outer regions of the disk around the collapsed star. It is easy to see that this luminosity is of the order of the residual optical/UV luminosity of LMXRTs. The expected values of the luminosity, L_{circ} , released by the mass transfer rate at the circularisation radius, r_{circ} , (see Lubow & Shu 1975) are given in Table 1. The mass transfer rate, \dot{M}_{tr} , of individual LMXRTs was estimated from binary evolutionary models (Pyllyer & Savonije 1988; King, Kolb & Burderi 1996), with the star masses and orbital period taken from Menou, Narayan & Lasota (1999). If this luminosity is released in the optically thick regime, equivalent black body temperatures of 6000–16000 K are expected. These temperatures and the values of L_{circ} are in the range measured for the residual optical/UV luminosity of LMXRTs. We emphasise that such an interpretation would hold even if an ADAF were present in the inner disk, provided the ADAF itself *does not* produce the bulk of the optical/UV emission; this is the case for the original ADAF model of Narayan et al. (1996; see Section 3).

Whether the emission at $\sim r_{\text{circ}}$ is azimuthally confined to the hot spot where the accretion stream from the mass donor impacts the outer disk was investigated by McClintock et al. (1983). These authors concluded that the modulation in the residual optical/UV flux of A 0620–00 may be consistent with that expected from the hot spot. Doppler maps (Marsh & Horne 1988) have been obtained for a number of quiescent BHC systems mainly by using the H α emission line and provide a further test for the geometry and kinematics of the accreting matter (Marsh, Robinson & Wood 1994; Casares et al. 1997; Harlaftis et al. 1996, 1997, 1999). These maps show the typical ring-like distribution of the outer regions of an accretion disk, similar to that observed in cataclysmic variables. The H α emission is strongest at a location associated with the interaction between the gas stream and the accretion disk, but extends also to a factor of ~ 2 higher velocity regions (*i.e.* somewhat smaller radii; e.g. Marsh et al. 1994).

The rate at which mass accumulates in the outer disk during quiescent intervals, \dot{M}_{acc} , has been estimated from the outburst recurrence time and fluence of those LMXRTs which have displayed more than one outburst (M99). Though uncertain, the inferred mass accumulation rate is of the order of the mass transfer rate from the companion star predicted by binary evolutionary models, \dot{M}_{tr} (in the context of ADAF models M99 adopt a value of

$$\dot{M}_{\text{acc}} \sim 1/3 \dot{M}_{\text{tr}}.$$

In consideration of the discussion in Section 3, we resolved to explore an alternative scenario for quiescent LMXRTs which does not involve an ADAF. Our basic ansatz is that during quiescence only a very small fraction of \dot{M}_{tr} (if at all) accretes onto the collapsed star, while a large fraction of \dot{M}_{tr} accumulates in the outer disk or is lost in a wind (e.g. Meyer-Hofmeister & Meyer 1999; Blandford & Begelman 1999). We are aware that such a sharp cutoff of the mass inflow rate from the outer disk regions is not envisaged by current instability models for LMXRTs. Yet, our suggested scenario is reminiscent of earlier (pre-ADAF) disk instability models that were proposed to explain the long recurrence time of A 0620–00 (Huang & Wheeler 1989; Mineshige & Wheeler 1989). These models are characterised by a very low mass transfer rate during quiescence (some ~ 8 orders of magnitude lower than at the outburst peak) and are capable of reproducing the ~ 50 yr outburst recurrence with an *ad hoc*, factor of ~ 20 , variation of the α viscosity parameter across the upper and lower branches of the surface density vs. viscosity relationship. We note that a similar scenario, namely a nearly empty inner accretion disk in quiescence, has been proposed to explain the delay between the rise of the optical/UV flux in cataclysmic variables within the disk instability models (e.g. King 1997). We also maintain that the swing between minimum and maximum mass inflow rates is similar across BHC and NS systems.

Our goal is to show that, if the mass inflow rate toward the compact object does vary by at least 7–8 orders of magnitude across the outburst/quiescence transition, then the properties of quiescent BHC and NS LMXRTs can be readily interpreted. This is done in the next two subsections.

4.1. Quiescent Black Hole Low Mass X-ray Transients

If the residual optical/UV luminosity of quiescent BHCs derives from the release of gravitational energy in the outermost disk regions by the material transferred from the companion star, then the faint quiescent X-ray luminosity of these systems might originate from very low level accretion onto the BHC, or, perhaps, from intense coronal activity in the outer disk region where matter accumulates.

For a standard radiative efficiency of ~ 0.1 , the observed X-ray luminosities would require that accretion into the BH takes place at a level of $\dot{M}_{\text{acc}} \sim 10^{11} - 10^{12}$ g s $^{-1}$ during quiescence. This value is 7–8 orders of magnitude lower than the mass accretion rate at the outburst peak and 2–4 orders of magnitudes lower than \dot{M}_{tr} , implying that only a minute fraction of the matter reaches the BHC in quiescence.

According to standard optically thick disk models, the emitted spectrum for a low mass inflow rate ($\lesssim 10^{14}$ g s $^{-1}$) onto a BH peaks at energies below 0.2 keV (e.g. de Kool 1988). However, if the density of disk becomes too low, thermal equilibrium can no longer be maintained and the accreting gas heats up giving rise to a hot phase in its innermost regions (de Kool & Wickramasinghe 1999). Such a hot inner corona may be responsible for the low level X-ray emission. In this interpretation the quiescent X-ray luminosity would be produced deep in the potential well ($\sim 10^7$ cm), *i.e.* a region $\sim 10^4$ smaller than R_{circ} .

Therefore uncorrelated X-ray and residual optical/UV luminosity variations might be expected.

An alternative, more speculative possibility involves coronal activity driven by shear and convection in the outer disk where matter accumulates. In this interpretation there would be virtually no mass accretion towards the BHC in quiescence (i.e. accumulation in the outer disk takes place without any significant leakage towards the BHC).

The analogy with the X-ray emission from K stars in RS CVn type binaries (which emit up to $\sim 10^{32}$ erg s $^{-1}$ in the ROSAT band; Dempsey et al. 1993) suggests that, in short orbital period BHC systems, such as A 0620–00, the low level X-ray quiescent luminosity ($\sim 10^{31} - 10^{32}$ erg s $^{-1}$) might also be due to coronal activity of the companion star (see also Bildsten & Rutledge 2000). In order to reach luminosities in excess of $\sim 10^{31}$ erg s $^{-1}$ a subgiant companion is required (Eracleous et al. 1991).

4.2. Quiescent neutron star Low Mass X-ray Transients

In this section we apply the scenario outlined above for BHCs to the case of NS LMXRTs. We first review the evidence that the NSs in these systems and, likewise LMXRBs, are fast spinning and weakly magnetic. We then explore the regimes spanned by such NSs as the mass inflow rate decreases and argue that radio pulsar shock emission, together with thermal emission from the NS surface, are responsible for the the quiescent X-ray emission of NS LMXRTs.

It had long been suspected that the NSs of persistent and transient LMXRBs have been spun up to very short rotation periods by accretion torques (Smarr & Blandford 1976; Alpar et al. 1982); however, conclusive evidence has been obtained only recently. The most striking case is that of SAX J1808.4–3658, a bursting transient source discovered with BeppoSAX in 1996 (in’t Zand et al. 1998). In April 1998, RossiXTE observations revealed a coherent ~ 401 Hz modulation, testifying to the presence of magnetic polar cap accretion onto a fast rotating magnetic NS (Wijnands & van der Klis 1998; Chakrabarty & Morgan 1998).

Millisecond rotation periods have also been inferred for 7 other LMXRBs of the Atoll (or suspected members of the) group through the oscillations that are present for a few seconds during type I X-ray bursts (for a review see van der Klis 1999). The spin frequencies inferred from burst oscillations span the range from 150 to 590 Hz, in agreement with the high spin frequency of millisecond radio pulsars (of which LMXRBs are likely progenitors). The ~ 550 , 525 and 150 Hz signal from Aql X-1, KS 1731–260 and the Rapid Burster, respectively, are the only burst oscillations revealed so far from LMXRTs.

Regarding the NS magnetic field, Psaltis & Chakrabarty (1999) estimate for SAX J1808.4–3658 a value of $B \sim 10^8 - 10^9$ G, by adopting different models for the disk-magnetosphere interaction. Indirect evidence for fields of $B \sim 10^8$ G derives also from the steepening in the X-ray light curve decay and marked change of the X-ray spectrum when the luminosity reaches a level of $\sim 10^{36}$ erg s $^{-1}$ in Aql X-1 (Campana et al. 1998b; Zhang et al. 1998)

²We use here simple spherical accretion theory. This is a reasonably accurate approximation when the accretion disk at the magnetospheric boundary is dominated by gas pressure, as in NS LMXRTs for a luminosity of $\leq 10^{36}$ erg s $^{-1}$. For a more general approach see e.g. Campana et al. (1998a).

and SAX J1808.4–3658 (Gilfanov et al. 1998), once these changes are interpreted in terms of the onset of the centrifugal barrier. It is still unclear whether such magnetic fields are strong enough that a small magnetosphere can survive when transient and persistent LMXRBs accrete close to their highest rate.

Accretion onto the surface of a magnetic NS can take place only as long as the centrifugal barrier of the rotating magnetosphere is open. In this regime, the accretion luminosity is given by $L(R) = GM\dot{M}/R$. Below a critical mass inflow rate \dot{M}_{cb} , corresponding to a luminosity of ²

$$L_{cb} \simeq 5 \times 10^{35} B_8^2 M_{1.4}^{-2/3} R_6^5 P_{2.5\text{ms}}^{-7/3} \text{ erg s}^{-1}, \quad (1)$$

($B = 10^8 B_8$ G, $P = 2.5 \times 10^{-3} P_{2.5\text{ms}}$ s, $R = 10^6 R_6$ cm and $M = 1.4 M_{1.4} M_\odot$ are the magnetic field, spin period, radius and mass of the NS, respectively) the magnetosphere expands beyond the corotation radius, r_{cor} , such that the centrifugal barrier closes, and the matter inflow stops at the magnetospheric radius, r_m , therefore releasing a lower accretion luminosity. The accretion luminosity gap, Δ_c , across the centrifugal barrier is (Corbet 1996):

$$\Delta_c = \frac{r_{cor}}{R} = \left(\frac{GM P^2}{4\pi^2 R^3} \right)^{1/3} \simeq 3 P_{2.5\text{ms}}^{2/3} M_{1.4}^{1/3} R_6^{-1}. \quad (2)$$

Δ_c depends almost exclusively on the spin period P and is basically a measurement of how deep r_{cor} is in the potential well of the NS.

Once the centrifugal barrier is closed, the NS enters the so-called propeller stage. It should be noted that the luminosity released by accretion in the propeller regime ($L(r_m) = GM\dot{M}/r_m$), is only a lower limit. An additional luminosity might be produced by: (a) matter leaking through the barrier (especially from the higher latitudes) and accreting onto the NS surface (Stella et al. 1986; Corbet 1996; Zhang et al. 1998); (b) the NS rotational energy released in the disk through the interaction with the magnetic field of the NS (e.g. Priedhorsky 1986). Moreover the fate of the bulk of the inflowing matter is uncertain as it may accumulate or be expelled by the action of the supersonically rotating magnetospheric boundary (Davies & Pringle 1981).

As the mass inflow rate decreases further the magnetosphere expands until the light cylinder radius, $r_{lc} = cP/2\pi$, is reached; beyond this point the radio pulsar dipole radiation will turn on and begin pushing outward the inflowing matter, due to a flatter radial dependence of its pressure compared to that of disk or radial accretion inflows (Illianorov & Sunyaev 1975; Stella et al. 1994; Campana et al. 1995). The equality $r_m = r_{lc}$ therefore defines the lowest mass inflow rate (and therefore accretion luminosity) in the propeller regime. An accretion luminosity ratio of

$$\Delta_p = \left(\frac{r_{lc}}{r_{cor}} \right)^{9/2} \simeq 440 P_{2.5\text{ms}}^{3/2} M_{1.4}^{-3/2} \quad (3)$$

characterises the range over which the propeller regime applies. Note that also this ratio depends mainly on the spin

period P . Once in the rotation powered regime, a fraction η of the spin down luminosity, L_{sd} , converts to shock emission in the interaction between the relativistic wind of the NS and the companion's matter flowing through the Lagrangian point. Theoretical models indicate that the material lost by the companion star may take somewhat different shapes, ranging from a bow shock to an irregular annular region in the Roche lobe of the NS, depending on radio pulsar wind properties and the rate and angular momentum of the mass loss from the companion star (Tavani & Brookshaw 1993; note that if a bow shock forms, which prevents material from accumulating in the Roche lobe of the compact object, the outburst activity might be inhibited permanently, see e.g. Shaham & Tavani 1991). The shock luminosity can be expressed as $L_{\text{shock}} = \eta L_{\text{sd}} \sim 6 \times 10^{31} \eta_{-1} B_8^2 P_{2.5\text{ms}}^4 \text{ erg s}^{-1}$ with η as large as 0.1 (Tavani 1991; $\eta \sim \eta_{-1} 0.1$). The luminosity ratio across the transition from the propeller to the rotation powered regime can be approximated as (Stella et al. 1994; Campana et al. 1998a)

$$\Delta_s = \frac{3}{2\sqrt{2}\eta} \left(\frac{r_g}{r_{\text{lc}}}\right)^{1/2} \simeq 2\eta_{-1}^{-1} P_{2.5\text{ms}}^{-1/2} M_{1.4}^{1/2}, \quad (4)$$

where $r_g = GM/c^2$ is the gravitational radius. Currently no prescription is available for the dependence of the shock-powered luminosity on the mass inflow rate. We note, however, that the 0.5–10 keV shock luminosity of the radio pulsar/Be star binary PSR 1259–63 varied by a factor of ~ 10 in response to the $\gtrsim 3$ orders of magnitude variation of mass capture rate at the accretion radius across its highly eccentric orbit (Hirayama et al. 1999). This suggests that the shock-powered luminosity depends only very weakly on mass inflow rate and, also in consideration of the uncertainties in the value of η , we will consider it a constant. The energy spectrum due to shock emission is expected to be a power law with photon index of $\sim 1.5 - 2$ that extends from a ~ 10 eV to ~ 100 keV, with both energy boundaries shifting as $B_8 P_{2.5\text{ms}}^{-3}$ (Tavani & Arons 1997; Campana et al. 1998a).

In summary, as the mass inflow rate towards a fast rotating weakly magnetic NS decreases, the ratio of the minimum luminosity from accretion onto the NS, L_{cb} , (just before the onset of the propeller effect) to the shock luminosity in the rotation powered regime is

$$\begin{aligned} \Delta_{\text{cps}} &\equiv \Delta_c \Delta_p \Delta_s \\ &= \frac{3}{2\sqrt{2}\eta} r_{\text{lc}}^4 r_{\text{cor}}^{-7/2} r_g^{1/2} R^{-1} \\ &\simeq 2 \times 10^3 \eta_{-1}^{-1} P_{2.5\text{ms}}^{5/3} M_{1.4}^{-2/3} R_6^{-1}. \end{aligned} \quad (5)$$

As expected Δ_{cps} depends almost exclusively on the spin period. On the contrary the absolute luminosity scale, set e.g. by L_{cb} , depends also on the NS magnetic field (see Eq. 1). It is easy to show that the variation of the mass inflow rate corresponding to Δ_{cps} can be expressed as

$$\dot{M}_{\text{cps}} \simeq 1 \times 10^2 P_{2.5\text{ms}}^{7/6} M_{1.4}^{-7/6}. \quad (6)$$

By combining Eqs. 1 and 5 with the Eddington luminosity, a lower limit is obtained on the minimum to maximum X-ray luminosity ratio of NS LMXRTs within the model

discussed here; this is (cf. Fig. 2)

$$\begin{aligned} \frac{L_{\text{min}}}{L_{\text{max}}} &> \frac{L_{\text{cb}}}{L_{\text{Edd}} \Delta_{\text{cps}}} = \frac{\eta L_{\text{sd}}}{L_{\text{Edd}}} \\ &\sim 2 \times 10^{-6} \eta_{-1} B_8^2 M_{1.4}^{-1} R_6^7 P_{2.5\text{ms}}^4. \end{aligned} \quad (7)$$

For the spin period and magnetic field inferred for NS LMXRTs this limit is consistent with the range of observed minimum to maximum X-ray luminosity ratios discussed in Section 2.2. On the contrary the minimum to maximum X-ray luminosity ratio inferred for BHC systems is substantially lower (see Section 2.1). The corresponding (minimum) mass inflow rate variation is given by

$$\frac{\dot{M}_{\text{cb}}}{\dot{M}_{\text{Edd}} \Delta \dot{M}_{\text{cps}}} \sim 3 \times 10^{-5} B_8^2 M_{1.4}^{-11/6} R_6^5 P_{2.5\text{ms}}^{-7/2}. \quad (8)$$

A 7–8 orders of magnitude variation of mass inflow rate from outburst to quiescence (see Section 4.1) would easily encompass this range. It should be noticed that two additional contributions to the quiescent X-ray luminosity of NS LMXRTs might be expected, the X-ray spectrum of which is thermal-like. An X-ray component in the $10^{32} - 10^{33} \text{ erg s}^{-1}$ range from the whole NS surface should be produced by the release of thermal energy from the NS interior heated up during the accretion episodes, unless a pion condensate is present in the NS core (Campana et al. 1998a; Brown, Bildsten & Rutledge 1998; Rutledge et al. 1999). Note that this might be relevant to both the propeller and the rotation powered pulsar regimes. Heating by relativistic particles associated with the radio pulsar emission might cause an additional soft X-ray quasi-thermal component from a much reduced area in the vicinity of the NS magnetic poles. The latter component is expected to be pulsed. The analogy with X-ray properties of the millisecond radio pulsars PSR J0437–4715 ($P = 5.8$ ms, $B = 3 \times 10^8$ G) and PSR J0218+4232 ($P = 2.3$ ms, $B = 4 \times 10^8$ G) suggests an X-ray luminosity from the polar caps in the $10^{30} - 10^{31} \text{ erg s}^{-1}$ range (Becker & Trümper 1999). The possible role of these emission components is further discussed in Section 5.

Fig. 2 illustrates the different emission regimes discussed in the previous sections for NS and BHC in LMXRTs as a function of the mass inflow rate. Accounting for the measured X-ray luminosity of quiescent BHCs (see Table 1) by means of standard ($\epsilon \sim 0.1$) accretion would require a very low accretion rate of $10^{-8} - 10^{-6} \dot{M}_{\text{Edd}}$. Any substantial X-ray flux from, e.g., coronal activity in the outermost disk regions would correspondingly decrease the required quiescent mass accretion rate into the BHC.

In the case of a NS system the different regimes are clearly seen for decreasing mass inflow rates: $L \propto \dot{M}$ when accretion onto the NS surface takes place; $L \propto \dot{M}^{9/7}$ from accretion onto the magnetospheric boundary in the propeller regime; $L \sim \text{const}$ in the radio pulsar shock emission regime. These regimes are separated by the gaps characterising the onset of the propeller and radio pulsar regimes. It is apparent from Fig. 2 that for a quiescent mass inflow rate of $\lesssim 10^{-5} \dot{M}_{\text{Edd}}$, the shock emission radio pulsar regime applies (cf. Eq. 8). Correspondingly, an X-ray luminosity of $\eta L_{\text{sd}} \sim 2 \times 10^{32} \eta_{-1} B_8^2 P_{2.5\text{ms}}^4 \text{ erg s}^{-1}$ would be expected, which is in the range measured from quiescent LMXRTs (cf. Eq. 7). It is also apparent from Fig. 2

that the X-ray luminosity swing predicted by our model is 1–2.5 decades smaller in NS than in BHC systems, if comparably large swings of mass inflow rates (in Eddington units) characterise the two classes of LMXRTs. This is also in agreement with the observations (see Section 2).

Incidentally, we note that in the relatively slow ($P \geq 1$ s) and high magnetic field ($B \sim 10^{12}$ G) NSs that are usually found in Be star X-ray transients, the centrifugal barrier sets in around $L_{\text{cb}} \sim 10^{35} - 10^{36}$ erg s $^{-1}$, Δ_c is a few hundreds and the propeller regime applies down to very low mass inflow rates ($\sim 10^{-6} - 10^{-7} \dot{M}_{\text{Edd}}$). For a plausible swing of mass inflow rate across the outburst to quiescence transition of Be transient systems, the resulting accretion luminosity swing is therefore expected to be many orders of magnitude larger than standard accretion theory would predict, without the NS ever entering the radio pulsar regime.

5. DISCUSSION

As emphasised in Section 4.2, the shock emission spectrum in the radio pulsar regime is expected to be a power law with photon index of $\Gamma \sim 1.5 - 2$. This is, at least qualitatively, in agreement with the hard power law like X-ray component observed in the quiescent X-ray spectrum of Cen X-4, Aql X-1 and X 1732–304. The extended power law spectrum expected from shock emission is also in agreement with the recently determined residual UV spectrum of Cen X-4, which shows no evidence for a turnover down to lowest measured UV energies (~ 7.5 eV) and matches quite well the extrapolation of the (power law) X-ray spectrum. We note that if the shock is located close to the circularisation radius (the most conservative case), an accretion luminosity in the $\sim 10^{32}$ erg s $^{-1}$ range would be released by the stream of matter from the companion, with a (black body) temperature of 7000–10000 K. This is, in turn, consistent with the idea that shock emission is at least comparable with the emitted spectrum in the blue and UV band, as expected in our model for typical NS parameters of LMXRTs. On the contrary quiescent state observations of the BHC LMXRT A 0620–00 show a marked steepening of the UV spectrum above ~ 5 eV, while the X-ray luminosity is one order of magnitude lower than that of Cen X-4.

Concerning the soft X-ray thermal-like component observed in the NS LMXRTs Aql X-1 and Cen X-4 (see Section 2.2), this accounts for about $\sim 60\%$ and $\sim 55\%$ of the total 0.5–10 keV quiescent luminosity, respectively. Therefore, the conclusions in Section 4.2 concerning the matching of the observed quiescent luminosity with the luminosity of the shock emission (power law) component remain essentially unchanged. We note that the effective black body radii inferred from spectral fitting of the soft component (~ 0.8 and ~ 3.1 km, respectively) are substantially smaller than the NS radius. However detailed, radiative transfer calculations for the NS atmosphere indicate that the emergent thermal-like X-ray spectrum is complex and simple black body fits are likely to underestimate the effective emission radius and overestimate the temperature by a factor of 3–10 and 2–3, respectively (Rutledge et al. 1999). Consequently, it cannot be ruled out yet that thermal emission from the whole NS surface powers the soft X-ray component of quiescent NS LMXRTs. Alternatively

heating of the magnetic polar caps by relativistic electrons might be responsible for the soft X-ray component observed from NS LMXRTs.

One might think of a propeller model in which the soft thermal-like component of the quiescent X-ray spectrum is indeed produced by cooling of the NS surface. In this case the requirement on the rate at which the inflowing matter reaches the NS magnetic pole could be relaxed (see M99), such that virtually 100% of the inflowing matter can be halted at the magnetospheric boundary. If we adopt a quiescent mass inflow rate that is $\sim 1/3$ of the binary mass transfer \dot{M}_{tr} (in analogy with the values deduced from ADAF modeling of quiescent BHCs, see M99), it is easy to see that for the values of $\dot{M}_{\text{tr}}/3 \sim 10^{15} - 10^{16}$ g s $^{-1}$ (10^{16} g s $^{-1}$ pertains to the longest orbital period BHCs) that are expected for NS systems, the luminosity produced in propeller regime by accretion onto the magnetosphere would be only a few times less efficient than accretion onto the NS surface, giving rise to a 2–3 orders of magnitude larger luminosity than observed (see Fig. 2). Such a model could be made marginally viable, only if accretion onto the magnetospheric boundary took a place in quiescent NS LMXRTs at rate a factor of ~ 100 smaller than $\dot{M}_{\text{tr}}/3$ (note that the relevant values of the mass inflow rate $\sim 10^{13} - 10^{14}$ g s $^{-1}$ would straddle the boundary between the propeller and the radio pulsar regime). However, this would require abandoning the idea that the swing of mass inflow rates is similar across BHC and NS systems.

We remark that if the radio pulsar/shock emission regime applies to quiescent NS systems, accretion towards the NS can resume only after the pressure of the accumulating material overcomes the radio pulsar pressure. This translates to a condition on the recurrence time of the outbursts

$$\Delta t \gtrsim 0.3 \dot{M}_{15}^{-1} h_9 T_4^{-1} B_8^2 P_{2.5\text{ms}}^{-4} \text{ yr} \quad (9)$$

where \dot{M}_{15} is the mass transfer rate from the companion in units of 10^{15} g s $^{-1}$, h_9 is the height of the outer disk in which matter accumulates in units of 10^9 cm and T_4 its temperature in units of 10^4 K. We note that the inferred outburst recurrence times of NS LMXRTs are indeed longer than Δt in the expression above for typical parameters. This, in turn, suggests that once the instability sets in, the radio pulsar pressure would be unable to halt the inflowing matter, and accretion can resume unimpeded.

6. CONCLUSIONS

The scenario we explored in this paper for the quiescent emission of LMXRTs assumes only very little matter (if at all) proceeds toward the collapsed object while most of the mass transferred from the companion star accumulates in an outer disk region or is lost in a wind. This idea is in line with models designed to explain the delays between the optical and UV light curves in the outbursts of cataclysmic variables. A suppression of the innermost disk regions (or nearly so) during quiescence is envisaged in those models as well (e.g. Livio & Pringle 1992; Meyer & Meyer-Hofmeister 1994; King 1997). Our suggested scenario is also reminiscent of earlier (pre-ADAF) disk instability models that were proposed to explain the long recurrence time of A 0620–00 within the context of stan-

standard accretion theory (Huang & Wheeler 1989; Mineshige & Wheeler 1989). At present we can only speculate on the reason why the quiescent outer disk would remain stable despite its effective temperature in $\sim 5000 - 10000$ K range. Perhaps the *ad hoc* variation of the α viscosity parameter that is required to make current disk instability models reproduce the outburst recurrence times (see Lasota & Hameury 1998) does not take place at the temperature at which the hydrogen ionisation and opacity change (as in current models), but rather at somewhat higher temperatures. In this case the outer disk region of quiescent LMXRTs could be in the lower branch of the corresponding surface density vs. viscosity relationship.

In our model the residual quiescent optical/UV emission (after subtraction of the contribution from the mass donor star) in BHC systems derives entirely from the gravitational energy released by the matter transferred from the companion star at radii comparable to the circularisation radius. The low quiescent X-ray luminosity originates either from standard accretion into the BHC at very low rates (some $\sim 10^{11} - 10^{12}$ g s^{-1}), and/or from coronal activity of the outer disk where matter accumulates or, limited to short orbital period systems, the companion star which is forced to corotate (see also Bildsten & Rutledge 2000). For comparably small mass inflow rates “leaking” from the outer disk regions, it can be safely concluded that the NSs of LMXRTs are in the radio pulsar regime, if their spin periods are a few millisecond and magnetic field some $\sim 10^8 - 10^9$ G, as indicated by the observations. The interaction of the radio pulsar relativistic wind with the matter transferred from the companion star gives rise to a shock, the power law like emission of which powers the harder X-ray emission component and optical/UV excess which are observed at a level of $\sim 10^{32} - 10^{33}$ erg s^{-1} in the quiescent state of Cen X-4. The soft, thermal-like component which contributes about half of the quiescent X-ray luminosity of several NS LMXRTs arises from the cooling of the NS surface in between outbursts or, perhaps, heating of the magnetic polar caps by relativistic particles in the radio

pulsar magnetosphere.

Both the X-ray and bolometric luminosity swing of BHC as well as NS systems are well matched by the model, for comparable ratios of minimum to maximum mass inflow rates toward the collapsed object across the two classes of LMXRTs. Moreover, different predictions are made about the quiescent emission of LMXRTs, which could be tested through higher spectral resolution and throughput observations to be obtained in the near future (e.g. with Newton-XMM). For example, if the quiescent X-ray emission of BHC systems resulted from coronal activity, emission lines from heavy elements and an optically thin thermal spectrum would be expected. Moreover residual optical/UV and X-ray flux variations should be correlated. On the contrary if a hot accretion disk with standard (as opposed to ADAF) efficiency gives rise to the X-ray flux, uncorrelated X-ray and residual optical/UV variations might take place. Variations in the optical/UV excess and the X-ray power law component of quiescent NS systems should be correlated, if they both arose from radio pulsar shock emission. The detection of pulsations at the NSs spin in the quiescent soft X-ray component would rule out emission from the whole NS surface and argue in favor of heated magnetic polar caps. The ultimate test of the radio pulsar regime in quiescent NS LMXRTs would be the detection of a pulsed radio signal. Yet, the matter in the outer disk and/or the shock might enshroud the pulsar making any radio signal very difficult to detect (Kochanek 1993; Stella et al. 1994; Campana et al. 1998a). The geometry of the radio pulsar shock and matter accumulating during the quiescent intervals of NS LMXRTs is highly uncertain; detailed Balmer line Doppler mapping (possibly at different times after the end of an outburst) could provide important clues on this issue.

This work was partially supported through ASI grants. LS acknowledges useful discussions with Luciano Burderi and Phil Charles. Paolo Goldoni provided useful comments on an earlier version of this manuscript.

REFERENCES

- Alpar M.A., Cheng A.F., Ruderman M.A. & Shaham J., 1982, *Nat* 300 728
 Asai K. et al., 1996, *PASJ* 48 257
 Asai K. et al., 1998, *PASJ* 50 611
 Becker W. & Trümper J., 1999, *A&A* 341 803
 Bildsten L. & Rutledge R.E., 2000, *ApJ* submitted (astro-ph/9912304)
 Blandford R.D. & Begelman M.C., 1999, *MNRAS* 303 L1
 Brown E.F., Bildsten L. & Rutledge R.E., 1998, *ApJ* 504 L95
 Campana S., 2000, in preparation
 Campana S., Colpi M., Mereghetti S., Stella L. & Tavani M., 1998a, *A&A Rev.* 8 269
 Campana S. & Stella L., Mereghetti S. & Colpi M., 1995, *A&A* 297 385
 Campana S. et al., 1998b, *ApJ* 499 L65
 Campana S. et al., 2000, submitted to *A&A*
 Cannizzo J.K., Wheeler J.C. & Ghosh P., 1985, in *Cataclysmic variables and low-mass X-ray binaries*, eds. D.Q. Lamb, & J. Patterson, Reidel, p 307
 Casares J., Charles P.A., Naylor T. & Pavlenko E.P., 1993, *MNRAS* 265 834
 Casares J., Martín E.L., Charles P.A., Molaro P. & Rebolo R., 1997, *New.A.* 1 299
 Chakrabarty D. & Morgan E.H., 1998, *Nat* 394 346
 Chen W., Shrader C.R. & Livio M., 1997, *ApJ* 491 312 (C97)
 Chevalier C., Ilovaisky S.A., Leisy P. & Patat F., 1999, *A&A* 347 L51
 Corbet R.H.D., 1996, *ApJ* 457 L31
 Davies R.E. & Pringle J.E., 1981, *MNRAS* 196 209
 de Kool M., 1988, *ApJ* 334 336
 de Kool M. & Wickramasinghe D., 1999, *MNRAS* 307 449
 Dempsey R.C., Linsky J.L., Flaming T.A. & Schmitt J.H.M.M., 1993, *ApJS* 86 599
 Eracleozzi M., Halpern J., Patterson J., 1991, *ApJ* 382 290
 Garcia M.R. & Callanan P.J., 1999, *AJ* 118 1390
 Garcia M.R., McClintock J.E., Narayan R. & Callanan P.J., 1998, in *Proceedings of the 13th North American Workshop on CVs*, eds. S. Howell, E. Kulkeers & C. Woodward, San Francisco AIP, in press (G98)
 Giles A.B., Hill K.M. & Greenhill J.G., 1999, *MNRAS* 304 47
 Gilfanov M., Revnivtsev M., Sunyaev R. & Churazov E., 1998, *A&A* 338 L83
 Guainazzi M., Parmar A.N. & Oostbroek T., 1999, *A&A* 349 819
 Hameury J.-M., Lasota J.-P., McClintock J.E. & Narayan R., 1997, *ApJ* 489 234
 Harlaftis E.T., Collier S., Horne K. & Filippenko A.V., 1999, *A&A* 341 491
 Harlaftis E.T., Horne K. & Filippenko A.V., 1996, *PASP* 108 762
 Harlaftis E.T., Steeghs D., Horne K. & Filippenko A.V., 1997, *AJ* 114 1170
 Hirayama M. et al., 1999, *ApJ* 521 718
 Huang M. & Wheeler J.C., 1989, *ApJ* 343 229
 in’t Zand J.J.M. et al., 1998, *A&A* 331 L25
 King A.R., 1997, *MNRAS* 288 L16
 King A.R., Kolb U. & Burderi L., 1996, *ApJ* 464 L127
 Kochanek C.S., 1993, *ApJ* 406 638

- Lasota J.-P., Hameury J.-M., 1998, in "Some Like it Hot!" S.S. Holt & T.R. Kallman eds., AIP Conference Proceedings 431, p.351
- Lasota J.-P., Narayan R. & Yi I., 1996, A&A 314 813
- Livio M. & Pringle J.E., 1982, MNRAS 259 L23
- Lubow S.H. & Shu F.H., 1975, ApJ 198 383
- Marsh T.R. & Horne K., 1988, MNRAS 235 269
- Marsh T.R., Robinson E.L. & Wood J.H., 1994, MNRAS 266 137
- McClintock J.E., Horne K. & Remillard R.A., 1995, ApJ 442 358
- McClintock J.E., Petro L.D., Remillard R.A. & Ricker G.R., 1983, ApJ 266 L27
- McClintock J.E. & Remillard R.A., 1986, ApJ 308 110
- McClintock J.E. & Remillard R.A., 2000, ApJ 531 956
- Menou K., Narayan R. & Lasota J.-P., 1999, ApJ 513 811
- Menou K. et al., 1999, ApJ 520 276 (M99)
- Meyer F. & Meyer-Hofmeister E., 1994, A&A 288 175
- Meyer-Hofmeister E. & Meyer F., 1999, A&A 348 154
- Mineshige S. & Wheeler C.J., 1989, ApJ 343 241
- Narayan R., Barret D. & McClintock J.E., 1997, ApJ 482 448
- Narayan R., Garcia M.R. & McClintock J.E., 1997, ApJ 478 L79 (N97)
- Narayan R., McClintock J.E. & Yi I., 1996, ApJ 457 821
- Orosz J.E. & Bailyn C.D., 1997, ApJ 477 876
- Orosz J.E. et al., 1998, ApJ 499 375
- Priedhorsky W.C., 1986, ApJ 306 L97
- Psaltis D. & Chakrabarty D., 1999, ApJ 521 332
- Pylyser E. & Savonije G.J., 1988, A&A 191 57
- Rutledge R.E., Bildsten L., Brown, E.F., Pavlov, G.G. & Zavlin V.E., 1999, ApJ 514 945
- Shaham J. & Tavani M., 1991, ApJ 377 588
- Shahbaz T., Bandyopadhyay R.M. & Charles P.A., 1999, A&A 346 82
- Shahbaz T., Casares J. & Charles P.A., 1997, A&A 326 L5
- Shahbaz T., Naylor T. & Charles P.A., 1993, MNRAS 265 655
- Shahbaz T. et al., 1998, MNRAS 300 1035
- Smarr L.L. & Blandford R., 1976, ApJ 207 574
- Spruit H.C., 2000, in "The neutron star black hole connection" (NATO ASI ELOUNDA 1999) ed. C. Kouveliotou et al. (astro-ph/0003143)
- Stella L., Campana S., Colpi M., Mereghetti S. & Tavani M., 1994, ApJ 423 L47
- Stella L., White N.E. & Rosner R., 1986, ApJ 308 669
- Stella L. et al., 2000, submitted to ApJ Letters
- Tanaka Y. & Shibazaki N., 1996, ARA&A 34 607
- Tavani M., 1991, ApJ 379 L69
- Tavani M. & Arons J., 1997, ApJ 477 439
- van der Klis M., 2000, submitted to ARA&A (astro-ph/0001167)
- van Paradijs J., 1996, ApJ 464 L139
- Wheeler J.C., 1996, in *Relativistic Astrophysics*, eds. W.H.G. Lewin, J. van Paradijs & E.P.J. van den Heuvel, (Cambridge Univ. Press), p 1
- Wijnands R.A.D. & van der Klis M., 1998, Nat 394 344
- Yi I. et al., 1996, A&AS 120 187
- Zhang S.N., Yu W. & Zhang W.W., 1998, ApJ 494 L71

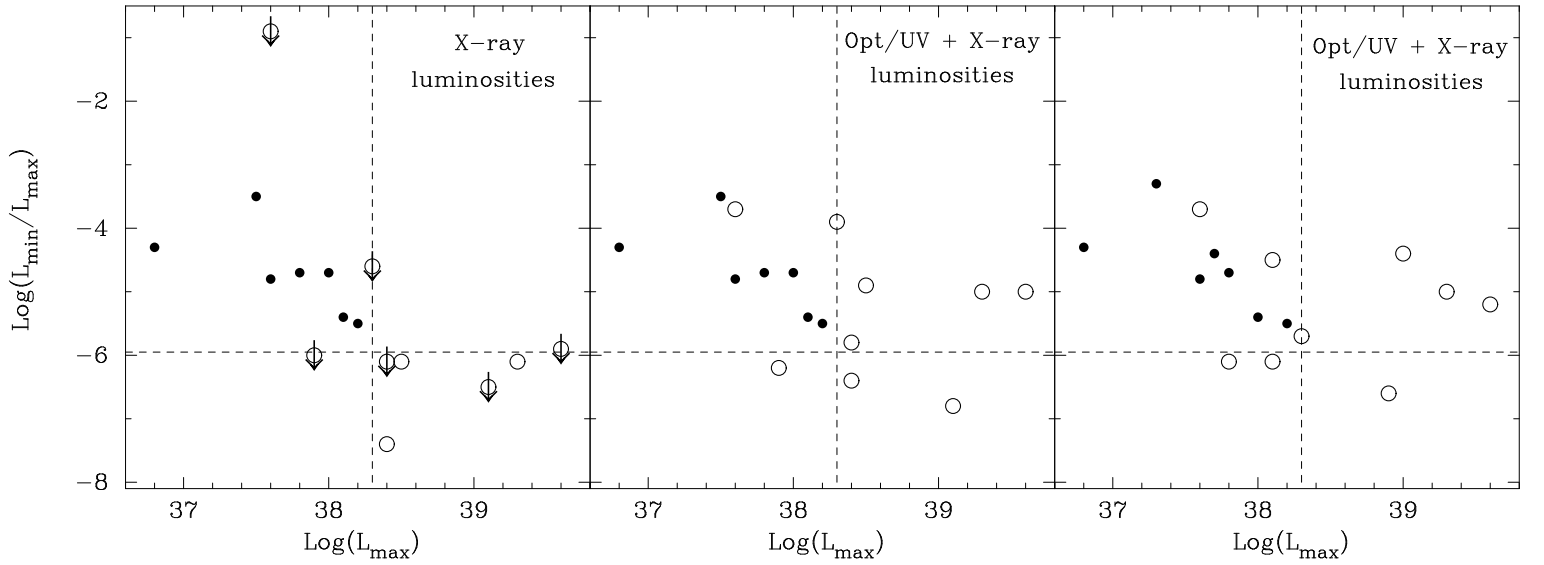


FIG. 1.— Minimum to maximum luminosity ratios versus maximum luminosity of NS (filled circles) and BHC (open circles) LMXRTs. The left panel shows the results based on the X-ray data alone ($L_{\text{min}}^X/L_{\text{max}}$). Arrows indicate upper limits. Maximum luminosities are according to G98. In the middle panel the luminosity ratio $L_{\text{min}}^{\text{bol}}/L_{\text{max}}$ includes the contribution of optical/UV photons (after subtraction the contribution of the companion star). The right panel is the same as the middle panel, except that the maximum luminosities estimated by C97 are used. Dashed lines represent the values of $L_{\text{min}}^X/L_{\text{max}}$ and L_{max} proposed by N97 to separate BHC from NS LMXRTs.

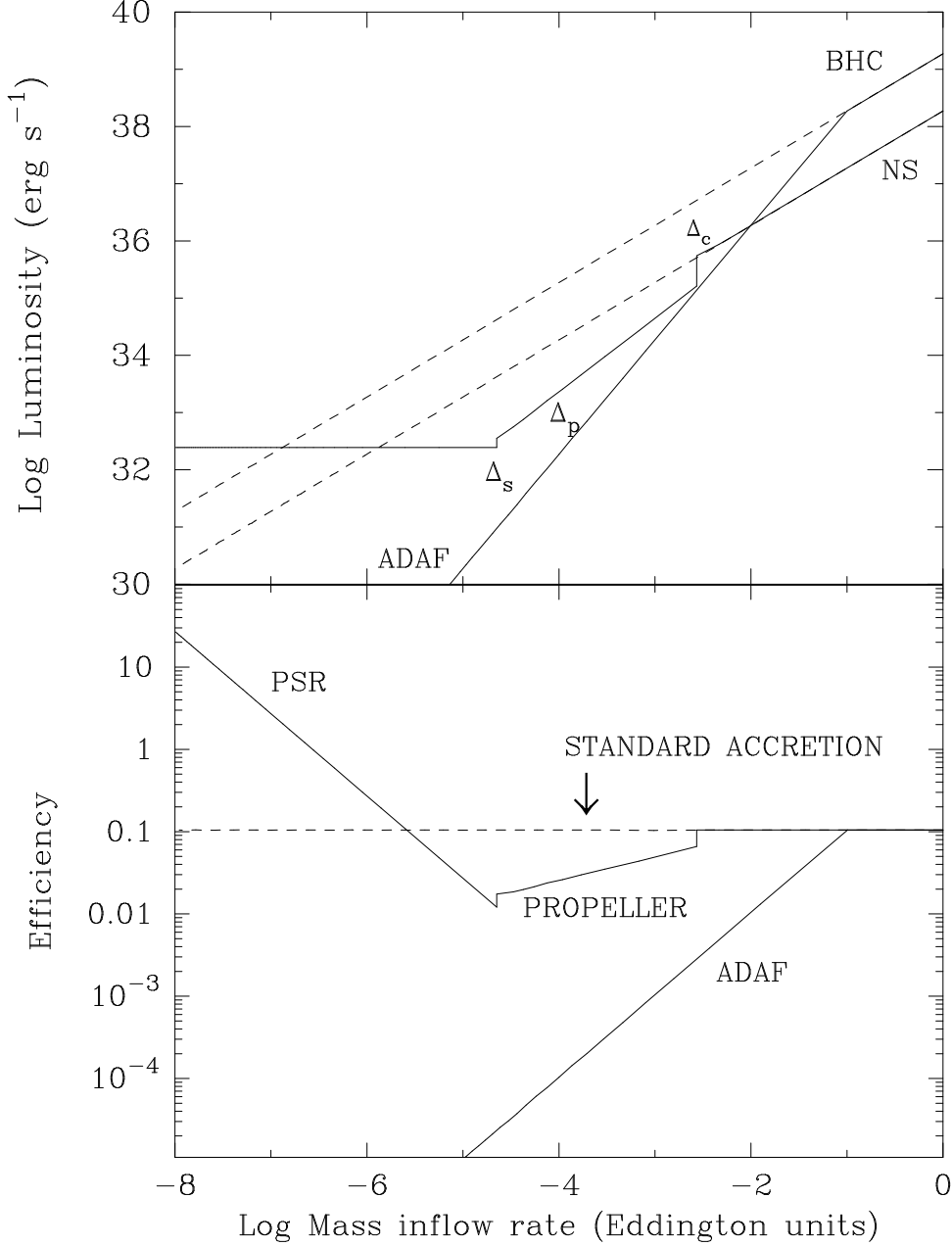


FIG. 2.— The upper panel shows the luminosity versus the mass inflow rate (in Eddington units $\dot{M} \sim 1.4 \times 10^{18} M/M_{\odot} \text{ g s}^{-1}$) for different accretion regimes onto BHs and NSs. The upper line refers to a $14 M_{\odot}$ BH. The dashed line marks the standard accretion regime (efficiency $\epsilon = 0.1$) and the continuous line the ADAF model. The lower lines refer to accretion onto a $1.4 M_{\odot}$ NS. The dashed line refers to accretion onto the NS surface. The continuous line gives the luminosity produced by a 2.5 ms spinning, $B = 10^8$ G NS in different regimes. The transition from the standard accretion regime ($L \propto \dot{M}$) to the regime of accretion onto the magnetospheric boundary in the propeller regime ($L \propto \dot{M}^{9/7}$; cf. Stella et al. 1994) and, subsequently, the radio pulsar shock emission regime ($L \sim \text{const}$) is clearly seen for decreasing mass inflow rates (see text). The lower panel gives the mass inflow to radiation conversion efficiency in the different regimes.